Available online at www.sciencedirect.com
ScienceDirect
Bioorganic & Medicinal Chemistry 15 (2007) 1795–1801
Bioorganic & Medicinal Chemistry

The dicationic derivatives of DBTAA: Interactions with DNA/RNA and antiproliferative effects on human cell lines

Marijana Radić Stojković,[a] Ivo Piantanida,[a,*] Marijeta Kralj,[b,†] Marko Marjanović,[b,†] Mladen Žinić,[a] Dariusz Pawlica[c,‡] and Julita Eilmes[c,‡]

[a]*Laboratory for Supramolecular and Nucleoside Chemistry, Division of Organic Chemistry and Biochemistry, Ruđer Bošković Institute, PO Box 180, HR-10002 Zagreb, Croatia*
[b]*Laboratory of Functional Genomics, Division of Molecular Medicine, Ruđer Bošković Institute, PO Box 180, HR-10002 Zagreb, Croatia*
[c]*Department of Chemistry, Jagiellonian University, Ingardena 3, 30-060 Kraków, Poland*

Received 8 September 2006; revised 15 November 2006; accepted 21 November 2006
Available online 29 November 2006

Abstract—Three dibenzotetraaza[14]annulenes non-covalently interacted with double-stranded DNA and RNA by mixed minor groove and/or intercalative binding mode. Observed interactions were strongly dependent on the steric exposure of positive charges and the length of the linkers of studied compounds as well as on the secondary structure and basepair composition of DNA/RNA. Compound **2** showed pronounced selectivity toward dA–dT-rich sequences and binding mode switch from dominant minor groove binding to ds-DNA to dominant intercalation into ds-RNA. Antiproliferative effect of studied compounds on human tumor and normal cell lines was in good agreement with the strength of observed interactions with DNA/RNA.

1. Introduction

Structural similarity to porphyrins, relatively easy synthesis, and rich chemistry[1] intrigued us to study dibenzotetraaza[14]annulenes (DBTAA). These tetraaza macrocycles are known for their ability to accommodate various substituents on the phenylene and diimine carbon atoms[2] and for tendency to adopt various conformations, ranging from planar to saddle shaped.[3] Furthermore, due to reactivity of their methine (*meso*) centers, fine tuning of physicochemical properties can be easily performed, as well as designing of their supramolecular behavior.[4] In addition, metal complexes of DBTAA offer a wide variety of coordination modes and geometries.[3,5] Although biological applications of porphyrins are most extensively studied,[6] particularly their interactions with DNA and RNA,[7] little is known about biological activity of dibenzotetraaza[14]annulenes and their metal complexes. Lack of data concerning their DNA/RNA binding properties prompted us to undertake such studies. Recently we have reported synthesis, crystal structures, and the preliminary evaluation of the new DBTAA-based DNA/RNA binding agents.[8] Three of these novel bis-cationic derivatives were subjected to more detailed study described in this paper (**1**–**3**, Fig. 1).

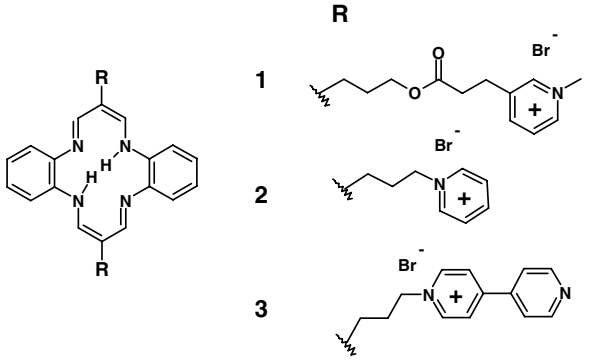

Figure 1. Bis-cationic derivatives of dibenzotetraaza[14]annulene (**1**–**3**).

Keywords: Antitumor agents; Dibenzotetraaza[14]annulenes; DNA sequence selectivity; Intercalation; Groove binding.
* Corresponding author. Tel.: +385 1 4571210; fax: +385 1 4680195 (I.P.); e-mail address: pianta@irb.hr; mhorvat@irb.hr; jeilmes@chemia.uj.edu.pl
† Tel.: +385 1 45 71 235; fax: +385 1 45 61 010.
‡ Tel.: +48 12 6632294; fax: +48 12 6340515.

0968-0896/$ - see front matter © 2006 Elsevier Ltd. All rights reserved.
doi:10.1016/j.bmc.2006.11.034

They contain positive charges at the end two spacers attached at the *meso* positions of the macrocycle to ensure approach to negatively charged phosphates of polynucleotide backbone. We have varied the length of linkers connecting DBTAA framework with cationic substituents, their chemical characters, and the structure of the moieties carrying positive charge. Our preliminary results[8] showed distinct non-covalent interactions of some of the novel compounds with ct-DNA. It appeared also that observed interactions were influenced remarkably by the bulkiness and rigidity of the pendant *meso* substituents. Since steric properties of a small molecule can control selective or even specific binding to different ds-DNAs and RNAs[9] and sometimes consequently control their biological activity, here we present more detailed study of interactions of the compounds **1**–**3** with various ds-DNAs and ds-RNAs. Their biological activities were also tested on a panel of human tumor and normal cell lines.

2. Results and discussion

2.1. Spectroscopic experiments

Spectroscopic properties of **1**–**3** and stability in aqueous solution were determined previously.[8] Similarly as observed before for ct-DNA,[8] addition of any ds-polynucleotide yielded strong bathochromic and hypochromic effects in UV/vis spectra of **1** and **2** but only very weak or no changes in the spectrum of **3** (Table 1).

It should be stressed that in all titrations of **2** with polynucleotides significant deviation from the isosbestic points was observed (e.g., Fig. 2), pointing toward coexistence of at least two different types of **2**/polynucleotide complexes. Titrations of **1** did not show any isosbestic points (which does not exclude nor prove that more complexes are formed).

Nice fitting of the UV/vis titration data to the Scatchard equation[10] gave binding constants (K_s) and ratios $n_{[\text{bound compound}]/[\text{polynucleotide}]}$ for the **1** and **2** (Table 2), while for **3** spectroscopic changes were too small for accurate processing. Calculated binding constants ($\log K_s$) and ratios n for **2** (Table 2) can be considered only as cumulative affinity of **2** toward polynucleotides since more types of complexes are formed. High values of ratio $n > 0.25$ obtained for **1** (Table 2) suggest that, most likely, **1** does not bind to polynucleotides by intercalation.[14]

The strong affinity of **2** toward all polynucleotides and strong bathochromic and hypochromic effects could be caused either by intercalation, minor groove binding or combination of both binding modes dependent on the **2**/polynucleotide ratio in the solution. From the titration data it was not possible to assume which binding mode prevails at UV/vis titration conditions (high

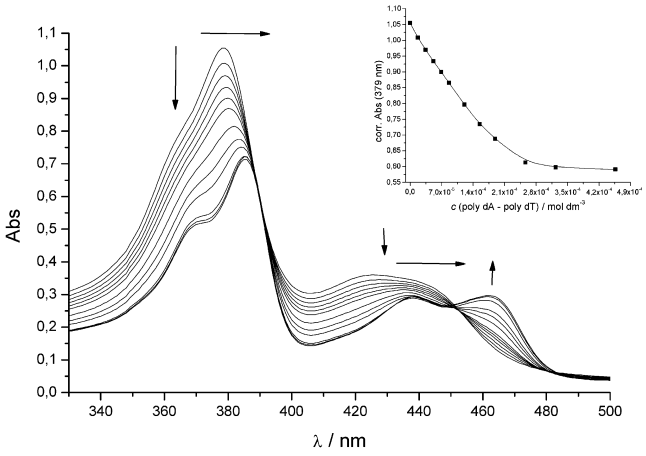

Figure 2. Changes in UV/vis spectrum of **2** ($c = 2.06 \times 10^{-5}$ mol dm^{-3}) upon titration with poly dA–poly dT; and dependence of **2** absorbance at $\lambda_{max} = 379$ nm on c(poly dA–poly dT), at pH 7, sodium cacodylate buffer, $I = 0.05$ mol dm^{-3}.

Table 1. Changes of **1**–**3** UV/vis spectra upon titration with ds-DNA and ds-RNA

		1	**2** ($I = 0.05$)	**2** ($I = 0.15$)	**3**
ct-DNA[c]	[b]H/%	−35	−46	−44	−8
	[a]$\Delta\lambda_1$	2	7	7	0
	[a] $\Delta\lambda_2$	8	9	9	2
poly dA–poly dT	[b]H/%	−48	−44	−47	−5
	[a]$\Delta\lambda_1$	2	6	6	0
	[a]$\Delta\lambda_2$	8	11	12	0
poly A–poly U	[b]H/%	−33	−43	−35	–
	[a]$\Delta\lambda_1$	2	8	8	1
	[a]$\Delta\lambda_2$	10	13	13	5
poly G–poly C	[b]H/%	−30	−35	−30	−11
	[a]$\Delta\lambda_1$	1	3	1	1
	[a]$\Delta\lambda_2$	7	9	7	4

[a] Shift of the absorbance maximum; $\Delta\lambda = \lambda$(complex) − λ(**1**, **2**, and **3**); Absorbance maxima λ_1 (**1**:$\lambda = 383$ nm, **2**:$\lambda = 379$ nm, **3**:$\lambda = 385$ nm) λ_2 = (**1**:$\lambda = 443$ nm, **2**:$\lambda = 427$ nm, **3**:$\lambda = 448$ nm).

[b] Hypochromic effect; H = (Abs(**1**,**2**,**3**) − Abs(complex))/Abs(**1**,**2**,**3**)) × 100; values Abs(complex) were calculated by Scatchard equation[10] for **1** and **2** and last experimental values were used for Abs(complex) of **3**.

[c] Reported previously.[8]

Table 2. Binding constants ($\log K_s$ and ratios n ([bound compound]/[polynucleotide phosphate]) calculated from the UV/vis titrations with ds-polynucleotides at pH 7.0 (buffer sodium cacodylate, $I = 0.05$ mol dm^{-3})[b]

		1 $I = 0.05$	**2** $I = 0.05$	**2** $I = 0.15$	**3** $I = 0.05$
ct-DNA[d]	$\log K_s$	5.2	4.7	4.24	[c]
	n[a]	0.69	0.84	0.54	[c]
poly dA–poly dT	$\log K_s$	5.3	6.1	4.77	[c]
	n[a]	0.38	0.099	0.27	[c]
poly A–poly U	$\log K_s$	5.9	5.19	5.4	[c]
	n[a]	0.42	0.45	0.15	[c]
poly G–poly C	$\log K_s$	6.1	4.2	—	[c]
	n[a]	0.57	1.7	—	[c]

[a] Accuracy of $n \pm 10$–30%, consequently $\log K_s$ values vary in the same order of magnitude.
[b] Titration data were processed according to the Scatchard equation.[10]
[c] Not possible to calculate by Scatchard equation due to the small spectroscopic changes.
[d] Reported previously.[8]

excess of polynucleotide binding sites over concentration of **2**). However, minor groove binding should depend more strongly on the electrostatic interactions than intercalation and therefore should be significantly more influenced by the substantial change of the ionic strength. Therefore, we have performed titration experiments with **2** at an order of magnitude higher ionic strength. Comparison of binding constants ($\log K_s$) (Table 2, $I = 0.15$) for analogous homo-polynucleotides showed that the affinity of **2** toward poly dA–poly dT is strongly affected by the ionic strength increase, while affinity of **2** to poly A–poly U virtually does not change. Former (DNA) homo-polynucleotide is characterized by narrow, deep, and hydrophobic minor groove,[11,12] which strongly supports minor groove binding of small molecules. On the other hand, minor groove of the latter homo-polynucleotide (RNA analogue) is shallow and broad,[13] inapt for the binding of small molecules.[9] Aforementioned results suggest that dominant binding mode of **2** to poly dA–poly dT is minor groove binding, while **2** binds to poly A–poly U mostly by intercalation.[14,15] Such a switch of the binding mode is quite common for a number of molecules characterized by structural features that enable binding to the polynucleotide by both binding modes.[9]

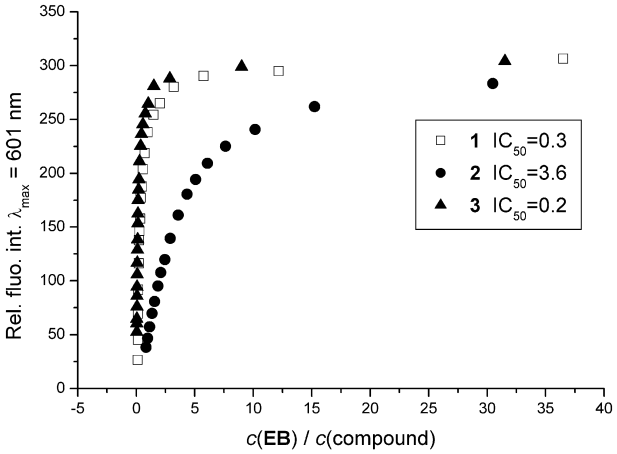

Figure 3. Ethidium bromide (**EB**) displacement assay: to ct-DNA solution ($c = 5 \times 10^{-5}$ mol dm^{-3}) ethidium bromide ($c = 5 \times 10^{-6}$ mol dm^{-3}) was added (r ([**EB**]/ [ct-DNA] = 0.1), and quenching of the **EB**/DNA complex fluorescence emission ($\lambda_{ex} = 520$ nm, $\lambda_{em} = 601$ nm) was monitored as function of c(**EB**)/c(compound). The given IC_{50} values present ratio c(**EB**)/c(compound) = [Int(**EB**/DNA) − Int($\mathbf{EB}_{free}$)]/2, where Int(**EB**/DNA) is fluorescence intensity of **EB**/DNA complex and Int($\mathbf{EB}_{free}$) is fluorescence intensity of the free ethidium bromide before DNA is added.

Since **2** and possibly **1** form simultaneously several different complexes with ds-polynucleotides and **3** did not yield large enough spectroscopic changes to determine binding constant (K_s), mutual comparison of the affinity of **1**–**3** toward ds-polynucleotides was inaccurate. Therefore, as an alternative method for estimation of affinity, at least as a comparison of ability of studied molecules to compete for binding with classical intercalator already bound to DNA,[16] we have performed ethidium bromide (**EB**) displacement assay (Fig. 3).

The obtained IC_{50} values (Fig. 3) show that more than one order of magnitude of **1** and **3** was needed to displace 50% of **EB** from ct-DNA than in the case of **2**. This finding does not directly correspond to the results of spectrophotometric titrations, which suggest comparable affinity of **1** and **2** to the most of the polynucleotides (Table 2). However, it should be taken into account that displacement of classical intercalator like **EB** does not necessarily mirror the cumulative affinity of compounds, which bind to the polynucleotides by mixed binding modes, as it was the case for **1** and **2**. In addition, titrations (Table 2) were done at high polynucleotide over compound excess, while ethidium bromide (**EB**) displacement assays were done in conditions close to the saturation of polynucleotide with compound.

Thus, to check results of ethidium bromide displacement assay under conditions close to the saturation of polynucleotide with compound, we have preformed thermal melting experiments (Table 3). Thermal stabilization effects of **1**–**3** on ds-polynucleotides (Table 3) agree well with the results of ethidium bromide displacement assay; both, ΔT_m and IC_{50} values are following the tendency $\mathbf{2} \gg \mathbf{1} > \mathbf{3}$. This tendency could be directly correlated with the bulkiness of peripheral substituents carrying positive charge as well as with the length, rigidity, and chemical character of the linkers. Thus, **2** having no substituent on the charged pyridinium ring and possessing

Table 3. ΔT_m values[a] (°C) of studied ds-polynucleotides upon addition of different ratios[b] r of **1**–**3** at pH 7.0 (buffer sodium cacodylate, $I = 0.05$ mol dm^{-3})

	r[b]	1	2	3
ct-DNA[c]	0.1	1.4	3.3	0
	0.2	1.5	5.0	0
	0.3	2.1	7.2	0
poly dA–poly dT	0.1	0.9	25.5	0.5
	0.2	5.9	29.0	3.0
	0.3	9.0	30.0	8.0
poly dAdT–poly dAdT	0.1	—	—	0.9
	0.2	—	—	1.3
	0.3	—	—	2.4
poly A–poly U	0.1	1.0	10.0	0
	0.2	1.0	14.3	0
	0.3	1.1	16.9	0.8

[a] Error in ΔT_m: ±0.5 °C.
[b] r = [compound]/[polynucleotide].
[c] Reported previously.[8]

the shortest and most flexible spacer is giving by far highest ΔT_m and IC_{50} values, **1** equipped with more bulky *N*-methylpyridinium groups linked via longer, more rigid, and significantly more polar spacers containing ester moiety is yielding significantly lower ΔT_m and IC_{50} values than **2**. Finally **3** having the most sterically demanding bipyridinium substituents did not stabilize ct-DNA and poly A–poly U at all, gave almost four times lower ΔT_m values for poly dA–poly dT compared to **2**, and yielded lowest IC_{50} value.

Only compound **2** yielded significant stabilization of the RNA homo-polynucleotide poly A–poly U, strongly supporting intercalation as the dominant binding mode.[9] Opposite to **2**, addition of **1** only weakly stabilized poly A–poly U suggesting prevalence of other binding modes than intercalation, possibly aggregation of the molecules in major groove of ds-RNA.

Compounds **1**–**3** induced significantly stronger thermal stabilization of poly dA–poly dT if compared with other polynucleotides. This observation could be correlated with peculiar secondary structure of poly dA–poly dT differing from structures of other ds-polynucleotides by specific narrow and deep minor groove.[11,12] Such a structure is convenient for efficient high affinity minor groove binding of small, hydrophobic, positively charged molecules. Of special interest is that **2** induced four times stronger thermal stabilization of poly dA–poly dT than observed for ct-DNA. Obviously, in the dG–dC-rich regions of ct-DNA, amino substituent on guanine positioned in minor groove[13] sterically hindered binding interactions and thus decreased stabilizing efficiency of **2**. That is in accordance with other minor groove binders showing dA–dT sequence preference.[9,17]

Since poly dA–poly dT was only polynucleotide stabilized by **3**, we have performed thermal melting experiments also with alternating poly dAdT–poly dAdT/**3** complex (Table 3). Although alternating dAdT polynucleotide was less stabilized than homo-polynucleotide (most likely due to the less narrow and hydrophobic minor groove), thermal stabilization was obviously higher than observed for ct-DNA, which was not stabilized at all. Alternating poly dAdT–poly dAdT and ct-DNA have quite similar secondary structure and the shape of the minor groove but differ significantly in basepair composition, ct-DNA consisting in high percentage of dG–dC basepairs. This observation is suggesting that **3** upon binding to minor groove selectively or even specifically stabilizes only dA–dT-rich regions (this is actually the reason of dA–dT sequence selectivity of many minor groove binding molecules).[9] Obviously, in the dG–dC rich regions of ct-DNA amino substituent on guanine positioned in minor groove[13] sterically hindered binding interactions and thus strongly hindered or even abolished stabilizing efficiency of **3**.

2.2. Biological assays

Since classical antitumor DNA-reactive drugs currently in the clinic display low sequence specificity, the growing interest emerges in novel sequence-specific small molecules that produce region-specific damage. Therefore, we also investigated the effects of **1**–**3** on proliferation of different human tumor cell lines, as well as on normal (diploid) human fibroblasts (control cell line), in order to determine their antitumor potential. Results presented in Table 4 show comparable effects induced by **1** and **2**, while addition of **3** did not yield any measurable activity. These observations are in good agreement with the results of spectroscopic titrations (Table 2) and also generally correspond to the results of the other methods.

The effect on the cell cycle perturbations as well as apoptosis activation was also measured on HeLa, MiaPaCa-2, and SW620 cells treated with **1** and **2** at the 5 μM concentration for 24, 48, and 72 h (Fig. 4). Remarkable changes in the cell cycle distribution of MiaPaCa-2 cells compared to the non-treated cells were noticed after the treatment with both **1** and **2**, which correlated perfectly with the cell proliferation assay.

Table 4. IC_{50} values (in μM)

	IC_{50}[a] (μM)					
	Cell lines					
	Hep-2	HeLa	MiaPaCa-2	SW 620	MCF-7	WI 38
1	38 ± 14	13.5 ± 4	2.6 ± 1.8	4.0 ± 1.3	2.6 ± 0.2	4.0 ± 2
2	11 ± 7	2.0 ± 1.9	1.2 ± 0.8	18.5 ± 2	6.0 ± 2.5	10 ± 6
3	>100	>100	>100	>100	⩾100	>100

[a] IC_{50}; the concentration that causes 50% growth inhibition.

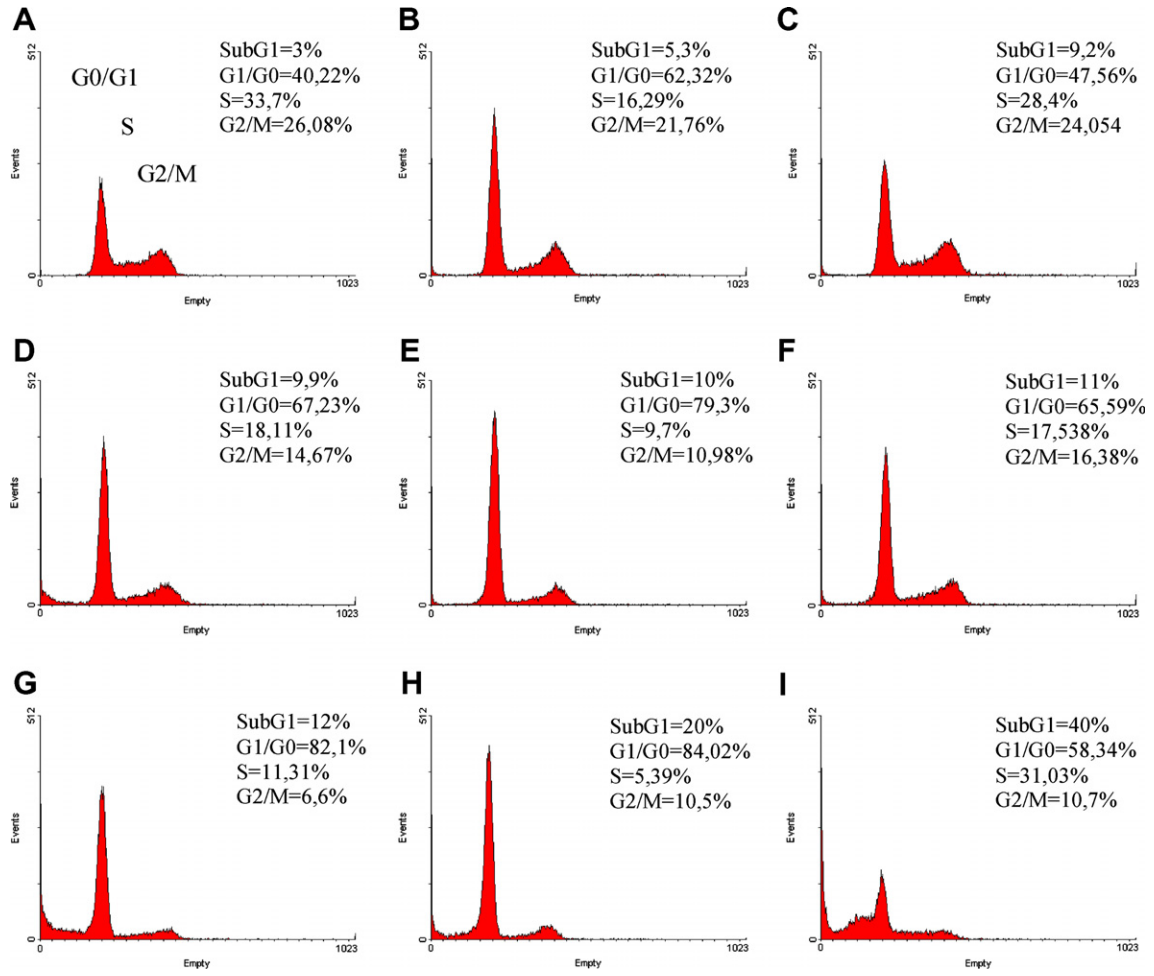

Figure 4. Effect of the compounds **1** (B, E, and H) and **2** (C, F, and I) on the cell cycle of MiaPaCa-2 cells. The cells were untreated (A, D, and G), or treated with 5 μM concentration of the compounds for 24 h (B and C), 48 h (E and F), and 72 h (H and I), fixed, and stained with propidium iodide to determine the DNA content. Percentage of the cells in each phase of the cell cycle was obtained by flow cytometric analysis. The percentages of apoptotic cells were confirmed by Annexin-V assay.

However, the effect of these two substances was quite different. Compound **1** induced strong accumulation of cells in G1, and reduction in S phase during first 48 h followed by the reduction of cells in G1 and S, accumulation in G2 phase, and a modest activation of apoptosis (confirmed by Annexin V assay, data not shown) after 72 h.

On the other hand, **2** did not induce dramatic changes within first 48 h, while it induced strong reduction of cell number in G1 and dramatic accumulation in S and G2/M phase, with marked induction of apoptosis after 72 h. However, much less evident effect on cell cycle and minor induction of apoptosis was noticed in HeLa and SW 620 cells by addition of both, **1** and **2** (data not shown). Different effects on tumor cell proliferation and/or cell cycle influences observed by the treatment with **2** may be due mostly to a different abundance of AT-rich sequences in various cell lines. For example, AT-rich sequences are found in regulatory regions in several cancer-related genes, such as c-Myc,[18] and it was shown that c-Myc is overexpressed in pancreatic cell lines.[19] Consequently, this could be the reason for higher sensitivity of MiaPaCa-2 cells (pancreatic carcinoma) to AT-selective derivative **2**. Moreover, significantly different effects on the cell cycle of MiaPaCa-2 cells could be explained by different structural features of **1** and **2** regarding the orientation of the positive charge. At biologically relevant conditions (high excess of DNA over compounds) the affinity of **1** is not AT-selective (Table 2); therefore it nonspecifically binds to DNA and inhibits replication in the first 48 h. On the other hand, **2** showed marked selectivity toward poly dA–poly dT compared to ct-DNA (Table 2), what is pointing toward possible accumulation of **2** in the AT-rich sequences, which could result in triggering different kinetic and/or mechanisms of action than **1**. Besides, AT-rich matrix attachment regions (MARs) contain consensus cleavage sites for topoisomerase II and since **2** induced strong S/G2/M arrest and apoptosis, after a prolonged period of time, topoisomerase inhibition as a mode of its action should be additionally confirmed.

3. Conclusions

Noncovalent interactions of **1**–**3** with ds-polynucleotides are strongly dependent on the size, rigidity, and structure

of positively charged substituents attached to macrocyclic moiety, as well as on the secondary structure of the ds-polynucleotides. Thus, compound **2** binds to polynucleotides by mixed binding mode; to DNA polynucleotides dominantly by minor groove binding, while to RNA analogues prevalently by intercalation. Upon binding to DNA, **2** showed strong selectivity toward dA–dT sequences, most likely due to the steric interference with the amino groups of guanines positioned into minor groove of dG–dC sequences. Compound **1** binds to polynucleotides mainly by groove binding, showing lower IC_{50} and ΔT_m values than **2**, most likely due to the longer, more rigid, and more polar linkers as well as to slightly different structure of the moiety carrying positive charge. Exceedingly bulky bipyridyl substituents of **3** markedly hampered interactions with polynucleotides, not allowing efficient aromatic π–π stacking interactions (that was reflected in small spectroscopic changes in UV/vis titrations), yielding lowest IC_{50} value, and weakly stabilizing exclusively AT-sequences of DNA polynucleotides. All these results point toward weak hydrophobic interactions of **3** exclusively within AT-sequences of DNA.

This is, to our knowledge, the first study that reports the biological activity of dibenzotetraaza[14]annulene-containing structures. The strength of the antiproliferative effect on cell lines (**1** ≈ **2** ≫ **3**) agreed well with the IC_{50} and ΔT_m values of **1**–**3** toward polynucleotides. Additionally, in the biological assays high excess of DNA over compound corresponds to the experimental conditions of titrations. Therefore, it is most likely that DNA is actually target of the compounds in the cell. Following the recently presented lead that AT-rich islands in genomic DNA can be considered as a target for AT-specific DNA-reactive antitumor drugs,[20] more detailed study of **1** and **2**, their metal complexes, and also close structural analogues is of the highest interest. Elucidation of mechanisms and significance of specific AT sequences targeting and their applicability to rational drug design is also of crucial importance.

4. Materials and methods

4.1. Spectroscopic experiments

Compounds **1**–**3** were prepared by the procedure described earlier.[8] The electronic absorption spectra were obtained on Varian Cary 100 Bio spectrometer in quartz cuvettes (1 cm). The spectroscopic studies were performed in aqueous buffer solution (pH 7, sodium cacodylate buffer, $I = 0.05$ mol dm^{-3}). Under the experimental conditions absorbance of **1**–**3** was proportional to their concentrations. Polynucleotides were purchased as noted: poly A–poly U, poly G–poly C, poly dA–poly dT, poly dAdT–poly dAdT (Sigma), calf thymus (*ct*)-DNA (Aldrich). Polynucleotides were dissolved in sodium cacodylate buffer, $I = 0.05$ mol dm^{-3}, pH 7. Calf thymus (ct)-DNA was additionally sonicated and filtered through a 0.45-μm filter.[21,22] Polynucleotide concentration was determined spectroscopically[22] as the concentration of phosphates. Spectroscopic titrations were performed by adding portions of polynucleotide solution into the solution of the studied compound.

Under the experimental conditions used the absorbance of **1**–**3** was proportional to their concentrations. Obtained data were corrected for dilution. Titration data were processed by Scatchard equation.[10] Values for K_s and n given in Table 2 all have satisfactory correlation coefficients (>0.999). Thermal melting curves for DNA, RNA, and their complexes with studied compounds were determined as previously described[22] by following the absorption change at 260 nm as a function of temperature. Absorbance of the ligands was subtracted from every curve, and the absorbance scale was normalized. The T_m values are the midpoints of the transition curves, determined from the maximum of the first derivative and checked graphically by the tangent method.[22] ΔT_m values were calculated subtracting T_m of the free nucleic acid from T_m of the complex. Every ΔT_m value here reported was the average of at least two measurements, the error in ΔT_m is ±0.5 °C.

4.2. Biological assays

4.2.1. Antiproliferative assays. The HeLa (cervical carcinoma), MCF-7 (breast carcinoma), SW 620 (colon carcinoma), MiaPaCa-2 (pancreatic carcinoma), Hep-2 (laryngeal carcinoma), and WI 38 (diploid fibroblasts) cells were cultured as monolayers and maintained in Dulbecco's modified Eagle's medium (DMEM) supplemented with 10% fetal bovine serum (FBS), 2 mM L-glutamine, 100 U/ml penicillin, and 100 μg/ml streptomycin in a humidified atmosphere with 5% CO_2 at 37 °C. The growth inhibition activity was assessed according to the slightly modified procedure performed at the National Cancer Institute, Developmental Therapeutics Program.[23,24] The cells were inoculated onto standard 96-well microtiter plates on day 0. The cell concentrations were adjusted according to the cell population doubling time (PDT): 1.5×10^4/ml for HeLa, Hep-2, MiaPaCa-2, and SW 620 cell lines (PDT = 20–24 h), 2×10^4/ml for MCF-7 cell lines (PDT = 33 h), and 3×10^4/ml for WI 38 (PDT = 47 h). Test agents were then added in five 10-fold dilutions (10^{-8}–10^{-4} mol l^{-1}) and incubated for further 72 h. Working dilutions were freshly prepared on the day of testing. After 72 h of incubation, the cell growth rate was evaluated by performing the MTT assay, as previously described.[23] Each test point was performed in quadruplicate in three individual experiments. The results are expressed as IC_{50}, which is the concentration necessary for 50% of inhibition. The IC_{50} values for each compound are calculated from dose–response curves using linear regression analysis.

4.2.2. Cell cycle analysis. The cells (2×10^5 per well) were seeded in a 6-well plate. After 24 h, the tested compounds were added at concentration 5×10^{-6} mol l^{-1}. After the desired length of time the attached cells were trypsinized, combined with floating cells, washed with phosphate buffer saline (PBS), and fixed with 70% ethanol. Immediately before the analysis, the cells were washed with PBS and stained with 1 μg/ml of propidium

iodide (PI) with the addition of 0.2 μg/μl of RNAse A. The stained cells were then analyzed with Becton Dickinson FACScalibur flow cytometer (20,000 counts were measured). The percentage of the cells in each cell cycle phase was determined using the ModFit LT software (Verity Software House Inc.) based on the DNA histograms. Statistical analysis was performed in SigmaStat 2.0 by using the one-way ANOVA test.

4.2.3. Annexin-V assay. Detection and quantification of apoptotic cells at single cell level was performed using Annexin-V-FLUOS staining kit (Roche), according to the manufacturer's recommendations. After the desired length of time, both floating and attached cells were collected. The cells were then washed with PBS, pelleted, and resuspended in staining-solution (annexin-V-fluorescein labeling reagent and propidium iodide (PI) in Hepes buffer). The cells were then analyzed under a fluorescence microscope. Annexin-V (green fluorescent) cells were determined to be apoptotic, and Annexin-V and PI cells were determined to be necrotic. Percentage of apoptotic cells was expressed as a number of fluorescent cells in relation to the total cell number (fluorescent and non-fluorescent cells), which was expressed as 100%.

Acknowledgments

Support for this study by the Ministry of Science, Education, and Sport of Croatia (Project 0098053) and by the Grant CRBW/44/2004 from the Jagiellonian University, Kraków, Poland, is gratefully acknowledged.

Supplementary data

Dose–response profiles for compounds **1**–**3** tested in vitro, along with more detailed explanation of antiproliferative assays. Supplementary data associated with this article can be found, in the online version, at doi:10.1016/j.bmc.2006.11.034.

References and notes

1. Mountford, P. *Chem. Soc. Rev.* **1998**, *27*, 105, and references therein.
2. Cutler, A. R.; Alleyne, C. S.; Dolphin, D. *Inorg. Chem.* **1985**, *24*, 2276.
3. Cotton, F. A.; Czuchajowska, J. *Polyhedron* **1990**, *9*, 2553.
4. (a) Hardie, M. J.; Malic, N.; Nichols, P. J.; Raston, C. L. *Tetrahedron Lett.* **2001**, *42*, 8075; (b) Malic, N.; Nichols, P. J.; Raston, C. L. *Chem. Commun.* **2002**, 16; (c) Eilmes, J.; Ptaszek, M.; Woźniak, K. *Polyhedron* **2002**, *21*, 7; (d) Eilmes, J.; Ptaszek, M.; Dobrzycki, Ł.; Woźniak, K. *Polyhedron* **2003**, *22*, 3299.
5. (a) Kofod, P.; Moore, P.; Alcock, N. W.; Clase, H. J. *J. Chem. Soc., Chem. Commun.* **1992**, *17*, 1261; (b) Ricciardi, G.; Bavoso, A.; Rosa, A.; Lelj, F.; Cizov, Y. *J. Chem. Soc., Dalton Trans.* **1995**, 2385; (c) Paul, R. L.; Gheller, S. F.; Heath, G. A.; Hockless, D. C. R.; Rendina, L. M.; Sterns, M. *J. Chem. Soc., Dalton Trans.* **1997**, 4143.
6. For reviews see e. g. Meunier, B.; Robert, A.; Pratviel, G.; Bernadou, J.. In *The Porphyrin Handbook*; Kadish, K. M., Smith, K., Guilard, R., Eds.; Academic Press: San Diego, CA, 1999; vol. 4, pp 119–187; Pandey, R. K.; Zheng, G.. In *The Porphyrin Handbook*; Kadish, K. M., Smith, K., Guilard, R., Eds.; Academic Press: San Diego, CA, 1999; vol. 6, pp 157–230.
7. (a) McMillin, D. R.; Shelton, A. H.; Bejune, S. A.; Fanwick, P. E.; Wall, R. K. *Coord. Chem. Rev.* **2005**, *249*, 1451; (b) McMillin, D. R.; McNett, K. M. *Chem. Rev.* **1998**, *98*, 1201; (c) Pasternack, R. F.; Gibs, E. J.; Villafranca, J. J. *Biochemistry.* **1983**, *22*, 2406; (d) Fiel, R. J. *J. Biomol. Struct. Dyn.* **1989**, *6*, 1259; (e) Fiel, R. J.; Howard, J. C.; Mark, E. H.; Datta-Gupta, N. *Nucleic Acids Res.* **1979**, *6*, 3093.
8. Pawlica, D.; Radić Stojković, M.; Sieroń, L.; Piantanida, I.; Eilmes, J. *Tetrahedron* **2006**, *62*, 9156.
9. Wilson, W. D.; Ratmeyer, L.; Zhao, M.; Strekowski, L.; Boykin, D. *Biochemistry* **1993**, *32*, 4098.
10. (a) Scatchard, G. *Ann. N.Y. Acad. Sci.* **1949**, *51*, 660; (b) McGhee, J. D.; von Hippel, P. H. *J. Mol. Biol.* **1976**, *103*, 679.
11. Nelson, H. C. M.; Finch, J. T.; Luisi, B. F.; Klug, A. *Nature* **1987**, *330*, 221.
12. Wilson, W. D.; Wang, Y. H.; Krishnamoorthy, C. R.; Smith, J. C. *Biochemistry* **1985**, *24*, 3991.
13. (a) Cantor, C. R.; Schimmel, P. R.. In *Biophysical Chemistry*; Freeman W.H. and Co. Ed.: San Francisco, 1980; vol. 3, p 1109; (b) Saenger, W. In *Principles of Nucleic Acid Structure*; Springer: New York, 1988.
14. Long, E. C.; Barton, J. K. *Acc. Chem. Res.* **1990**, *23*, 271.
15. Dougherty, G.; Pilbrow, J. R. *Int. J. Biochem.* **1984**, *16*, 1179.
16. Boger, D. L.; Fink, B. E.; Brunette, S. R.; Tse, W. C.; Hedrick, M. P. *J. Am. Chem. Soc.* **2001**, *123*, 5878.
17. Wilson, W. D.; Tanious, F. A.; Buczak, H.; Venkatramanan, M. K.; Kumar, A.; Boykin, D. W.; Munson, R. In *Structure and Function*. In *Nucleic Acids*; Sarma, R. H., Sarma, M. H., Eds.; Adenine Press: New York, 1992; vol. 1, pp 83–105.
18. Woynarowski, J. M.; Napier, C.; Trevino, A. V.; Arnett, B. *Biochemistry* **2000**, *39*, 9917.
19. Han, H.; Bearss, D.; Browne, W.; Calaluce, R.; Nagle, R. B.; Von Hoff, D. D. *Cancer Res.* **2002**, *62*, 2890.
20. Woynarowski, J. M.; Trevino, A. V.; Rodriguez, K. A.; Hardies, S. C.; Benham, C. J. *J. Biol. Chem.* **2001**, *276*, 40555.
21. Chaires, J. B.; Dattagupta, N.; Crothers, D. M. *Biochemistry* **1982**, *21*, 3933.
22. Palm, B. S.; Piantanida, I.; Žinić, M.; Schneider, H. J. *J. Chem. Soc., Perkin Trans. 2* **2000**, 385.
23. Jarak, I.; Kralj, M.; Šuman, L.; Pavlović, G.; Dogan, J.; Piantanida, I.; Žinić, M.; Pavelić, K.; Karminski-Zamola, G. *J. Med. Chem.* **2005**, *48*, 2346.
24. Boyd, M. R.; Paull, K. D. *Drug Dev. Res.* **1995**, *34*, 91.